Advanced Materials Research Vols. 133-134 (2010) pp 1233-1239

doi:10.4028/www.scientific.net/AMR.133-134.1233

Experimental Research on Seismic Behavior of Non-Rigid Steel Beam-Column Connections with Concrete Cover

JIANG Lixue[1,2,a], ZHOU Feng[1,2,b] and ZHENG Qiaowen[1,2,c]

[1] Shanghai Research Institute of Building Sciences, Shanghai, China

[2] Shanghai Key Laboratory of New Technology for Engineering Structures, Shanghai, China

[a]jianglixue@sohu.com, [b]zhougf@gmail.com, [c]qiaowenzheng@hotmail.com

Abstract Four steel beam-column connections were tested under cyclic loads to investigate effects of the concrete cover and the cast-in-situ slabs on the failure modes, stiffness, load-carrying capacity, ductility and energy-dissipation capacity. The test results show that the stiffness and bending strength of the non-rigid steel connections are significantly increased due to the presence of concrete cover and the cast-in-situ slabs can further enhance the connections. Moreover, the connection with slab is prone to debonding failure along beam-slab interface resulting in a remarkable decrease of the stiffness and strength. Practical methods are also presented for analyzing and assessing the steel frames with non-rigid connections considering effects of concrete cover.

Keywords: Steel frame, non-rigid beam-column connection, seismic behavior, stiffness, load-carrying capacity.

Introduction

Many middle-high-rise historic buildings, which are steel frames and constructed in the first half of 20th century, are still in service in some Chinese cities, such as Shanghai and Tianjing. These aged steel frames are very different from present high-rise steel structures in design principle and connection detailing. No seismic design was taken into account and wind-resistant design was also experience based. Most steel connections were fastened by the means of rivets and could be regarded as semi-rigid. Steel structural members were often wrapped by concrete or bricks for protection purpose. These historic buildings are basically in good conditions after seventy or even eighty years' service, even though the strength and stiffness for these structures are seriously inadequate according to the current design method (GB50010-2002, GB50011-2001). It is believed that the underestimate of the performance of structures are mainly caused by neglecting the effect of non-structural components, such as infilled wall and wrapped cover (Jiang et al. 2005). Actually, concrete cover can increase the stiffness of steel structural member as well as the rotational rigidity and the strength of steel connections.

Many researches have been conducted on the non-rigid connections of steel frames (Chen et al. 2003, Wang et al. 2003, Xiao et al. 1994), but few considered the interaction of the non-rigid connections and concrete cover. In view of these situations, experimental study on the composite non-rigid connection was conducted to investigate the effects of concrete cover and slabs on the failure mode, stiffness, load-carrying capacity, ductility and energy-dissipating capacity of connections.

Test Scheme

The full-scale test specimens were designed based on the typical exterior connections of the Bank of China Building located at the Bund in Shanghai (Jiang et al. 2005). To simplify the fabrication,

H-shape steel was adopted and rivets were replaced by bolts. Each specimen consisted of a 2m long steel beam with section of I500×200×10×16 and a 3.2m long column with section of I400×400×13×21, as shown in Fig. 1. The ordinary bolts of grade 5.6, size M20 were used for all fasteners. Specimens J3 and J4 were wrapped by 50mm thickness concrete cover (C15 fine aggregate concrete). Specimen J4 included a 120mm thick slab extending by 3.8m in the direction of the orthogonal beams (with section of I400×200×8×13). Φ12 and ϕ8 steel bars were placed at the top and bottom of the slab in loading direction with 200mm and 150mm spacing respectively. ϕ10 and ϕ8 steel bars were placed at the top and bottom of the slab in orthogonal direction with 150mm spacing. All the specimens are shown in Fig. 1 and Table 1.

Table 1: Specimen list

Specimens	*Description*
J1	Basic specimen. The column flange and the beam web were bolted with double angles.
J2	Comparing with Specimen J1, the connection was strengthened by adding T-stubs between the column flange and the beam flanges.
J3	Same as Specimen J1 and wrapped by concrete cover.
J4	Same as Specimen J3, and concrete slab and orthogonal beams were added.

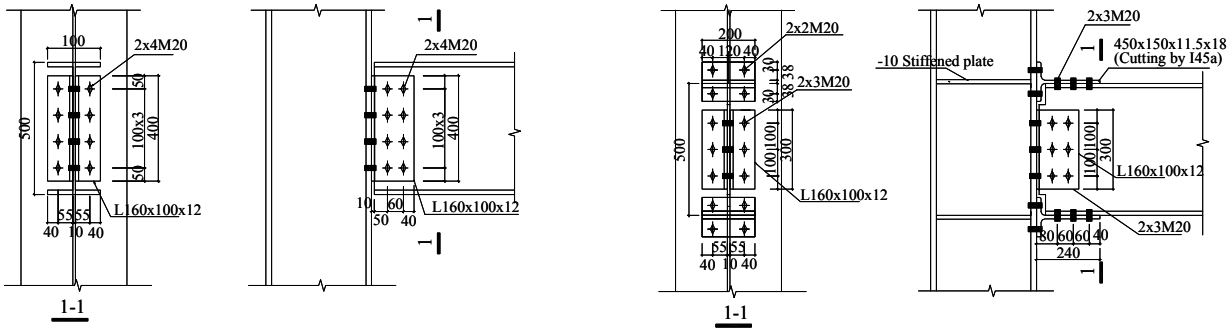

(a) Details of Specimen J1

(b) Details of Specimen J2

(c) Dimensions of beam and column of Specimen J3

(d) Slab of Specimen J4

Figure 1: Test specimens

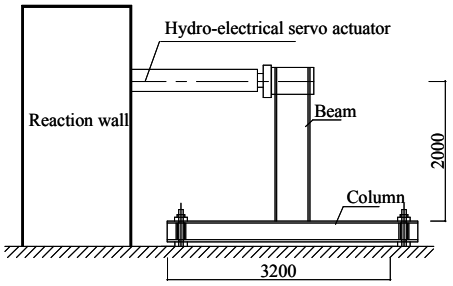

Figure 2: Test setup

(a) J1 (b) J4

Figure 3: View of test specimens

For the convenience of test setup, the column of the specimens was placed horizontally, and quasi-static cyclic loads were applied by a hydro-electrical servo actuator at the end of the cantilever beam, as shown in Fig.2 and Fig.3. Both ends of the column were fixed through anchor bolts on the floor, and no axial load was applied on the column. The test started by using the load control and converted to the displacement control after the specimen yielded.

Test Results and Analysis

Material Properties The cube strength of concrete for specimens J3 and J4 were 19.3 and 20.1MPa, respectively. Material properties of H-shape steel and steel bar are shown in Table 2.

Table 2: Material properties

Items	*Yielding strength [MPa]*	*Tensile strength[MPa]*	*Elasticity Modulus[$\times 10^5$MPa]*
Beam flange plate (16mm)	315	425	—
Beam web plate (10mm)	370	480	—
steel bar(Φ12)	378	525	2.05

Mechanical Behavior and Failure Mode The column flange and the beam web of Specimen J1were bolted with double angles and this kind of connection is normally regarded as a pinned joint. When the end of beam was cyclically loaded, the angles bore tension and compression alternatively. When under compression, the angles were pushed and contacted with the column flange. When under tension, the angles were uplifted from the column face. When the displacement of the beam end reached 120mm, the bolts at the first outer row loosed, and the bolts on the column (the bolts under tension) loosed earlier than the bolts on the beams (the bolts under shear). The plastic elongation of the bolts under tension was notable. When the displacement of the beam end reached 160mm, the angle leg adjacent to the fillet fractured. The crack propagated with the increase of the load and displacement. The failure mode of Specimen J1 is shown in Fig. 4(a). The major damage and plastic deformation of the specimen concentrated on the angles and blots, and no significant damage was found on the beam and the column.

Specimen J2 Specimen J2 was strengthened by adding T-stubs between the column flange and the beam flanges. This kind of connection is normally regarded as a rigid connection. Under the cyclic loading, plastic deformation of the specimen concentrated on the T- stubs connections. When the displacement of the beam end reached 40mm, the bolts on the T-stubs and the angles loosed gradually, and the bolts on the T-stubs under tension elongated plastically. When the displacement of the beam end reached 80mm at the second cycle, one of the bolts on T-stubs fractured by tension and the load resistance of the specimen decreased significantly. The failure mode of Specimen J2 is shown in Fig. 4(b). It can be found that most of the bolts on T-stubs in tension fractured, and the bolts which didn't fail had significant plastic elongations or loosed. The connection and the T-stubs had residual deformation, while the other parts of beam and column remained almost intact after the loading.

Specimen J3 Specimen J3 was same as Specimen J1 and wrapped by concrete cover. When the load reached 52kN, the first bending crack appeared near the root of the beam (close to the column face). When the displacement of the beam end reached 12.5mm, the crack width reached 1mm. When the displacement reached 25mm, several cracks appeared, and the width of the first crack increased to 5mm. When the displacement reached 90mm, the concrete near the root of the beam crushed. The failure mode of Specimen J3 is shown in Fig. 4(c). It can be found that the concrete of the beam nearly detached from that of the column, and the crack width at the connection reached 30 to 50 mm. Significant residual deformation on the beam can also be observed.

Specimen J4 Further to Specimen J3, concrete slab and orthogonal beams were added for Specimen J4. The load was defined as positive load when the top surface of the slab is under tension, and vice versa. The first crack on root of the beam and on the top surface of the slab

appeared when the load reached -15kN and 50kN, respectively. When the beam end displacement reached -15mm, cracks were found at the interface between the beam and the slab. When the displacement reached 45mm, the cracks at the interface progressed through the length of the beam. When the displacement reached -60mm, cracks appeared on the bottom surface of the slab. The concrete at the root of the beam crushed after the displacement reached 100mm. The failure mode of Specimen J4 is shown in Fig. 4(d). It can be found that the beam was almost totally separated from the slab. The beam end was seriously damaged by cracking and crushing. More cracks were found on the bottom surface of the slab than on the top surface, since the slab only bore the negative load after the slab and the beam detached.

(a) J1 (b) J2 (c) J3 (d) J4

Figure 4: Failure modes of the specimens

Hysteresis Behavior of the Specimens The load-deformation relationships of the 4 specimens are shown in Fig. 5, where P and Δ represent the applied load and the horizontal displacement at loading point, respectively. The hysteresis curves of Specimen J1 and J3 were stable and repetitive. The load and stiffness of Specimen J2 significantly decreased after the bolts on the T-stubs fractured. The ultimate deformation capacity is limited. The hysteresis curve of Specimen J4 was stable when the specimen bore negative load. When the specimen bore positive load, the load decreased significantly after the beam and the slab detached. After that, the hysteresis curve can be supposed to only represent the performance of the beam (without the slab). All hysteresis curves show pinch effect obviously, since plastic deformation often concentrated on the connection, and the beams and the columns deformed elastically. Therefore, the energy dissipation capacity of the specimens is limited.

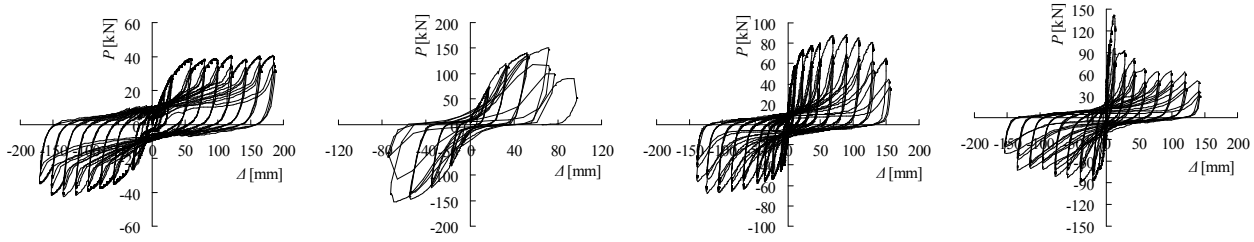

(a) J1 (b) J2 (c) J3 (d) J4

Figure 5: Load-displacement relationships of the specimens

Load Capacity, Displacement and Ductility The load capacity, displacement and ductility factor of each specimen are listed in Table 3. The skeleton curves are shown in Fig. 6.

The stiffness and load carrying capacity of Specimen J1 was limited while the deformation capacity was large. When the displacement of the beam end reached 180mm (i.e., drift angle was 1/11), the specimen still could bear the maximum positive load and reduced slightly for negative load. The ductility factor was more than 2.5. The structural performance of the double-angle connection as a pinned joint is reflected.

The stiffness and load carrying capacity of Specimen J2 were much larger than that of Specimen J1. Its average ultimate load capacity in two loading direction is 3.7 times that of Specimen J1. But the deformation capacity and ductility of Specimen J2 were worse than that of Specimen J1. Ultimate deformation is defined as the displacement when the load decreased to 85% of the peak

load. Ultimate deformation capacity of Specimen J2 was less than half of the Specimen J1's. The ductility factor was about 2. In the aged steel frame, the stiffness and strength of beam-column connection was less than that of steel beam, so plastic deformation often concentrated on the connection and the bolts. When the beam drift angle reached 1/25, the plastic elongation on the bolts of T-stubs needed to be more than 15mm (i.e., elongation ratio is 50%). The bolts could not bear such high elongation, so they fractured earlier, and the load carrying capacity of the connection decreased. It revealed the superiority of the rigid connection in the stiffness and strength as well as its deficiency in deformation capacity.

Table 3: Load capacity, displacement and ductility of each specimen

Specimens	Load direction	Yielding point			Ultimate load point			Ultimate displacement point			Displacement ductility factor
		Load [kN]	Displacement [mm]	Drift angle	Load [kN]	Displacement [mm]	Drift angle	Load [kN]	Displacement [mm]	Drift angle	
J1	+	34.60	46.30	1/43	38.97	58.94	1/29	40.00	184.26	1/11	3.98
	−	-35.27	-64.60	1/31	-42.62	-133.79	1/15	-36.23	-165.82	1/12	2.57
J2	+	125.9	39.96	1/50	151.44	71.33	1/28	128.22	80.04	1/25	2.00
	−	-129.61	-39.72	1/50	-151.68	-69.07	1/29	-138.5	-71.29	1/28	1.79
J3	+	73.28	22.68	1/88	88.26	88.84	1/23	73.26	139.19	1/14	6.14
	−	-53.02	-23.51	1/85	-67.46	-122.56	1/16	-57.05	-134.37	1/15	5.72
J4	+	123.20	8.50	1/235	141.36	12.23	1/164	120.16	20.6	1/97	2.42
	−	-73.00	-10.84	1/185	-88.81	-38.66	1/52	-76.55	-86.48	1/23	7.98

Note: the drift angle represents the ratio of the displacement of the beam end to the beam length.

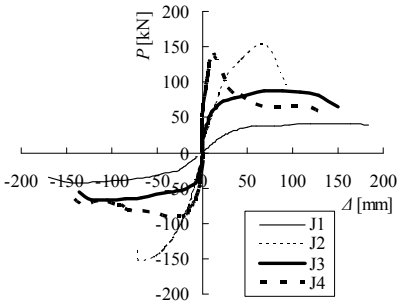

Figure 6: Skeleton curves of load-displacement relationship

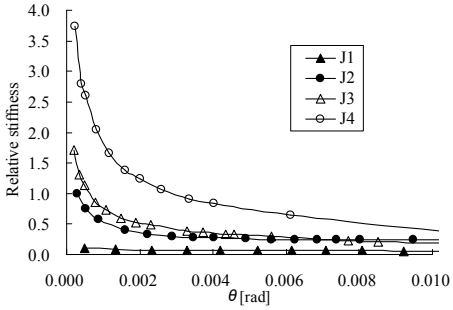

Figure 7: Stiffness degradation curves

The load carrying capacity of Specimen J3 is about 1.9 times that of J1 but less than that of J2. It should be pointed out that the larger resistance under positive load was caused by the thicker concrete layer of the top of beam (Fig. 1(c)). The ductility and deformation capacity of Specimen J3 was better than that of J2. The ultimate drift angle was 1/15 and ductility factor was close to 6.

The initial stiffness of J4 was larger than that of other specimens. The load carrying capacity of J4 under positive load (when the top surface of the slab is under tension) was 141kN, which is 3.5 times that of J1 and similar with that of J2. Its load carrying capacity under negative load is more than twice that of J1 and close to that of J3 under positive load. It is found that the reinforcement in the slab is beneficial to increase load carrying capacity under positive load, if the shear capacity of the interface between beam and slab are reliable. Since no shear connectors were adopted between the concrete slab and the steel beam, shear strength of the interface was very low. The debonding failure occurred along beam-slab interface early and diminished the composite action, resulting in significant decrease of the stiffness and strength. The ultimate drift angle under positive load was only 1/97, and less than that of other specimens. The ultimate drift angle under negative load was 1/23 and the ductility factor was close to 8. The ultimate deformation and the ductility under negative load are better than that under positive load because of the debonding failure.

Strain on the End of Steel Beam Strain gauges were glued on the top and bottom flanges of steel beams at a distance of 280mm from the column face. The test results revealed that the maximum longitudinal strain of Specimen J1, J3 and J4 (pinned joint) was less than ±300με, reflecting a low utilization coefficient of the material strength of steel beam. The maximum longitudinal strain of Specimen J2 (rigid connection) ranged from -800 to 600με, reflecting an increased utilization coefficient of material. Since the beam flange didn't yield, the material strength was not fully used.

Connection Stiffness and Degradation Trend Initial stiffness of each specimen is listed in Table 4. The initial stiffness of Specimen J2 was about 8.9 times that of J1. The initial stiffness of J3 was 1.72 times that of J2 because of the effect of the concrete cover. The initial stiffness of J4 reached to 3.74 times that of J2 because of the effect of the concrete slab.

The composite section of the beam and column of Specimen J3 could be converted to the equivalent cross section of concrete. Assumed that the connection was a concrete connection, the initial stiffness was calculated as 57470 kN/m, which was between the initial stiffness of J3 and J4 obtained in the experiments. Based on that, the double-angle connection with concrete cover and slab as Specimen J4 can be treated as a rigid connection and the initial stiffness can be estimated based on a concrete connection with equivalent cross section.

The stiffness degradation curves of each specimen are shown in Fig. 7. Except for Specimen J1, the stiffness degradation for all specimens was very notable. When the drift angle of the beam reached 1/500, the stiffness of J1, J2, J3 and J4 reduced to 65%, 35%, 30% and 33% of the initial stiffness, respectively. When the drift angle of the beam reached 1/50, the stiffness of J1, J2, J3 and J4 further reduced to 50%, 18%, 6% and 3% of the initial stiffness, respectively.

Table 4: Initial stiffness of specimens

Specimens	*Tested initial stiffness [kN/m]*	*Relative initial stiffness*	*Corresponding beam rotation[$\times 10^{-3}$]*
J1	2020	0.11	0.49
J2	17982	1.00	0.28
J3	30923	1.72	0.20
J4	67236	3.74	0.22

Note: relative initial stiffness represents the ratio of the initial stiffness of each specimen to that of J2.

Connection bending strength analysis To calculate the bending strength of the connection, following assumptions were adopted based on the test results: (1) the bolts had the same material properties with the beam flange; (2) the strain of the bolts, compressed concrete and tensile reinforcement in the slab could be estimated using the plane cross-section assumption based on the drift angle of the beam end; (3) for steel specimen, the compressive capacity of the connection was calculated on the condition of full contact of the junction plate under compression; (4) the specimen with concrete cover and slab could be regarded as concrete member, and the bending capacity could be evaluated based on that the tension blots and concrete were treated as tensile reinforcement and compression zone, respectively. The effective width of slab was also considered. The calculated and tested flexure strength of each specimen are shown in Table 5, and matched well with each other.

Table 5: Tested and calculated flexure strength of each specimen

Specimen	*Tested flexure strength[kN·m]*	*Calculated flexure strength [kN·m]*	*Ratio*
J1	77.94	68.25	0.88
J2	302.88	295.74	0.98
J3	176.52	166.48	0.94
J4	282.72	257.39	0.91

Note: Tested flexure strength represents the flexure strength measured under the positive load.

Conclusions

Four steel beam-column connections were tested under cyclic loads to investigate the effects of the concrete cover on the seismic performance of non-rigid connections. The test results can be concluded as follows.

(1) The stiffness and strength of the double-angle connection is limited, but the deformation capacity is good. It can be treated as pinned joint in structural design. Double-angle adding T-stub connection can be treated as rigid connection. The stiffness and strength are much higher than that of double-angle connection. But the deformation often concentrates on the joint and the bolts fracture by tension easily, so the energy dissipation and deformation capacity is limited.

(2) The concrete cover significantly increases the stiffness of non-rigid connections. The initial stiffness of J3 was 15.6 and 1.72 times that of J1 and J2, respectively. The improvement in stiffness will gradually diminish with the development of concrete cracks. The concrete slab further enhances the stiffness of non-rigid connections. The initial stiffness of J4 was 34 and 3.74 times that of J1 and J2, respectively.

(3) The internal moment arm of the section is increased by considering the compression zone of concrete cover and the bending capacity of the connection is increased accordingly. The strength of J3 was 1.9 times that of J1. Due to the contribution from the tensile reinforcement in the slab, the concrete slab further enhances the strength of connections. The strength of J4 was 3.5 times that of J1. Since the shear bond strength between the concrete slab and the steel beam was unreliable, debonding failure along slab-beam interface occurs easily and the stiffness and strength decrease significantly.

(4) It is suggested that the non-rigid connection of steel frames with concrete cover and slab could be regarded as rigid connection in structural appraiser. Initial stiffness could be calculated based on the steel-concrete composite section. The load-carrying capacity could be estimated based on the equivalent cross section of concrete, while the blots and concrete were treated as tensile reinforcement and compression zone respectively, and the contribution of the tensile reinforcement of the slab should not be considered.

Acknowledgement

The financial support from the National Key Technology R&D Program (Grant No. 2006BAJ03A10) is greatly acknowledged.

References

[1] Chen, A G, Gu, Q, Su, M Z, and Li, Q C (2003). "Cyclic behavior of double angle beam-column connections." *Journal of Building Structure*, 24, 31-35 (in Chinese).

[2] *Code for design of concrete structures (GB50010-2002)*, Beijing,2002.

[3] *Code for seismic design of buildings (GB50011-2001)*, Beijing,2001.

[4] Jiang, L X, Hu, S L, and Zhu, C M (2005). "Safety and seismic appraisal of the Bank of China building at the Bund of Shanghai." *Building Structure*, 35, 3-6 (in Chinese).

[5] Wang, Y, Li, H J, and Li, J F (2003). "Initial Stiffness of semi-rigid beam-column connections and structural internal force analysis."*Journal of Engineering Mechanics*,20,65-69(in Chinese).

[6] Xiao, Y, Choo, B S, and Nethercot, D A (1994). "Composite connections in steel and concrete. I. Experimental behavior of composite beam-column connections." *Journal of Constructional Steel Research*, 31, 3-30.